

WKB approximation to bosonic dark matter

Lauren Street,^{*} Peter Suranyi,[†] and L.C.R. Wijewardhana[‡]
Department of Physics, University of Cincinnati

Galactic dark matter halos may be composed of ultralight axions (ULAs) ($m_a \lesssim 1$ eV) with wave functions that satisfy nonlinear Schrödinger-Poisson equations (SPA). We find eigenstates of SPA in WKB approximation. The expansion parameter of the WKB approximation is $\delta = 1/\sqrt{S}$, where $S = 2MRGm_a^2$, with M being the total mass, R the radius of the halo, and G the gravitational constant. $S \gg 1$ for almost all galaxies, even if the ULA mass is as small as $m_a = 10^{-22}$ eV, making the leading order WKB approximation almost exact. As the level spacing of bound states is roughly proportional to δ , the number of states in the gravitational well is huge. We do not see a reason why not all or most of them contribute to the halo. Using an appropriate distribution function allows the summation of states to construct the profile of the halo as a function of the gravitational potential, which can be found solving the Poisson equation. Using various energy distribution functions, we obtain results similar to those in simulations. Future plans include investigations of collapse through time dependent generalizations, and inclusion of self-interactions, which also induce decay processes of the halo.

arXiv:2308.11094v1 [astro-ph.GA] 22 Aug 2023

^{*} streetlg@mail.uc.edu

[†] peter.suranyi@gmail.com

[‡] rohana.wijewardhana@gmail.com

The structure of galaxies and the rotation curves of stars in galaxies can potentially be explained with the assumption that most of galactic matter is composed of presently unknown particles, termed dark matter (DM), which interact very weakly with particles of the Standard Model. One of the most popular variants of DM is the weakly interacting massive particle (WIMP), consisting of massive, non-relativistic particles, heavier than neutrinos [1–3]. Since no such particles, in the appropriate mass range, have been discovered yet, other alternatives for DM have also been considered. Among others, a prominent candidate is ultralight axions (ULAs) with Compton wavelengths ranging from cosmic size [4–14] to that of masses $m_a \sim 1$ eV [15].

There have been many simulations of the collapse of ULAs on galactic scales without [16–22] and with baryonic feedback [23]. In both cases, ULA systems were shown to collapse to a condensed core, surrounded by a virialized halo of non-relativistic ULA. Recently, there have also been simulations performed for ULAs with self-interactions, [24–26], for systems composed of multiple flavors without self-interactions [27], and for systems composed of multiple flavors with self-interactions [28]. In order to study dynamic perturbations to the central soliton, multiple eigenstates of a Schrodinger Poisson system where the gravitational potential for higher modes is generated by the solitonic ground state was performed in reference [29]. These states can be used to construct halos of low mass galaxies where due to the low value of S only a small number of states contribute to the halo.

In another work [30], self-consistent simulations of the halo constructed from excited states of the Schrödinger-Poisson (SP) equations were performed. The authors found that the collapse of the system consisted of a condensed soliton core surrounded by a halo composed of excited eigenstates. In a subsequent work [31], systems satisfying SP equations were analyzed assuming composition of a small number of energy eigenstates, including the stability and virialization of the system.

The purpose of this work is to construct DM from self-adjoint or complex ULAs with self-interactions using WKB approximation. We ignore self-interactions in solving the equations of motion, but in a subsequent work we will consider the effect of $2 \rightarrow 2$ interactions on the stability of excited eigenstates. We emphasize that, because only this particular interaction is relevant, our model can be used for real, or just as easily for complex, scalar fields. For the sake of simplicity, we focus on a real scalar field giving rise to a ULA subject to a Φ^4 self-interaction. Such an interaction is the leading order expansion term of an axion potential, $V = m_a^2 f^2 [1 - \cos(\Phi/f)]$. For the range of galactic sizes and ULA masses considered here, the contribution of self-interaction terms to the equations of motion is negligible compared to that of the gravitational interaction. The ratio of self-interactions to gravitational interactions scales as

$$\frac{SI}{GI} \sim \frac{M_P^2}{f_a^2} \frac{1}{m_a^2 R^2},$$

where $M_P = G^{-1/2}$ is the Planck mass and G is Newton's constant, f_a is the axion decay constant, R is the radial scale of the system and m_a is the mass of the axion. Using $m_a = 10^{-22} \text{eV}$, $f/M_p = 10^{-3}$ for the Milky Way with $R = 10^5$ light year, we obtain $SI/GI \simeq 10^{-4}$.

Self-interactions of ULAs may be important for extremely small galaxies. In fact, based on studies of axion stars [32–34] they can possibly generate a cutoff in the mass of small, stable galaxies with very large densities. That possibility will be investigated in future publications.

I. EQUATIONS OF MOTION

Our basic assumption is that radial eigenfunctions of the halo satisfy a Schrodinger-Gross-Pitaevskii equation

$$E_{nl}\psi_{nl} = -\frac{1}{2m_a} \left[\psi_{nl}'' + \frac{2}{r}\psi_{nl}' \right] + \left[\frac{1}{2m_a} \frac{l(l+1)}{r^2} + V_g \right] \psi_{nl}, \quad (\text{I.1})$$

where quantum numbers n and l characterize eigenstates, and V_g is the gravitational potential. The most general stationary state wave function of the halo is

$$\Psi(\mathbf{r}, t) = \sum_{nlm} \psi_{nl}(r) Y_{lm}(\theta, \phi) e^{i(E_{nl}t + \alpha_{nlm})}, \quad (\text{I.2})$$

where α_{nlm} are random phases. Then the gravitational potential is

$$V_g = -G m_a \int d^3 r' \frac{\Psi(\mathbf{r}')^2}{|\mathbf{r} - \mathbf{r}'|} \simeq -G m_a \sum_{nl} (2l+1) \int d^3 r' \frac{\psi_{nl}(r')^2}{|\mathbf{r} - \mathbf{r}'|}, \quad (\text{I.3})$$

where we average over time and random phases, and assume spherical symmetry.

The main result of this paper is the analytic derivation of the density distribution of a ULA halo. Suppose the gravitational potential of the system, $V_g(r)$, is known. Then the density distribution satisfies the Poisson equation

$$\nabla^2 V_g(r) = -4\pi G m_a \rho(r). \quad (\text{I.4})$$

If we can construct the density distribution as a function of V_g , then Eq. (I.4) constitutes a second order differential equation for V_g which can be solved, providing the density distribution. This density distribution can then be compared to simulations or observations.

Expanding the wave function in radial coordinates, assuming again that interference terms are negligible when taking averages and the density distribution is spherically symmetric, the number density can be written as

$$\rho(r) = m_a \sum_{nl} (2l+1) |\psi_{nl}|^2, \quad (\text{I.5})$$

where we normalize wave functions as

$$\int d^3r |\psi_{nl}|^2 = N_{nl}, \quad (\text{I.6})$$

where $N_{nl} \equiv M_{nl}/m_a$ and M_{nl} is the total mass of states having quantum numbers n and l .

In phenomenological models ([35, 36]) the central density and radial scale are undetermined free parameters. To compare various radial scales we introduce the universal radial scale parameter R , the rescaled dimensionless coordinate, $z = r/R$, and the gravitational scaling function, $w(z)$, through the equation

$$V_g(z) = -G \frac{m_a^2}{R} \int d^3z' \frac{\tilde{\rho}(z')}{|z-z'|} = -\frac{GM m_a}{R} w(z), \quad (\text{I.7})$$

where we rescale the density as $\tilde{\rho}(z) = (R^3/m_a) \rho(r)$. Choosing R as the harmonic average of r weighted over the density,

$$\frac{1}{R} = \left\langle \frac{1}{r} \right\rangle, \quad (\text{I.8})$$

the gravitational potential at the center is $V_g(0) = -GM m_a/R$. Then Eq. (I.7) implies that $1 \geq w(z) > 0$, with $w(0) = 1$.

Phenomenological models of halos are of the form $\rho(r) = \rho(0)f(r/R_s)$, where R_s is a radial scale, differing from the one defined in Eq. (I.8). The concentration is defined as $c = r_{\text{vir}}/R_s$, the virial radius, r_{vir} , is usually defined as the radius of a sphere containing the total mass of the halo and densities are cut off at r_{vir} .

Using our method, all densities vanish at some finite value of $z = z_{\text{vir}}$ which we identify with the scaled virial radius, $z_{\text{vir}} = r_{\text{vir}}/R$. In phenomenological models, the scales of models, e.g. concentration, are not universal between models. As Eq. (I.8) implies $\langle 1/z \rangle = 1$, we can give a universal definition to the concentration $c = z_{\text{vir}}$.

Note that R is of the same order of magnitude but larger than the scaling parameter of phenomenological models ([35, 36]) and unlike those, *model independent*. That can be shown by calculating the harmonic average, Eq. (I.8), in those models. The harmonic radius of a NFW halo is

$$R = R_{\text{NFW}} \left[\left(1 + \frac{1}{c_{\text{NFW}}} \right) \log(1 + c_{\text{NFW}}) - 1 \right] > R_{\text{NFW}}, \quad (\text{I.9})$$

where R_{NFW} is the scaling radius of the NFW halo, and c_{NFW} is the NFW concentration. Similarly, the harmonic radius of the Burkert halo is

$$R = R_{\text{B}} \frac{\log(1 + c_{\text{B}}^2) + 2 \log(1 + c_{\text{B}}) - 2 \tan^{-1}(c_{\text{B}})}{\log(1 + c_{\text{B}}^2) - 2 \log(1 + c_{\text{B}}) + 2 \tan^{-1}(c_{\text{B}})} > R_{\text{B}}, \quad (\text{I.10})$$

where R_{B} is the scaling radius of the Burkert halo, and c_{B} is the Burkert concentration.

Another interesting property of the gravitational scaling function, $w(z)$ is related to its behavior at the virial radius. Virial radius is defined by $w(z_{\text{vir}}) = 0$. Taking Eq. (I.7) at $z = z_{\text{vir}}$ and using Gauss's theorem we obtain

$$V_g(z_{\text{vir}}) = -\frac{GM m_a}{r_{\text{vir}}} = -\frac{GM m_a}{R z_{\text{vir}}} = -\frac{GM m_a}{R} w(z_{\text{vir}}), \quad (\text{I.11})$$

with the implication $w(z_{\text{vir}}) = 1/z_{\text{vir}}$.

We also define rescaled dimensionless wave functions, with unit normalization, as

$$\phi_{nl}(z) = R^{-3/2} N_{nl}^{1/2} \psi_{nl}(r). \quad (\text{I.12})$$

Writing Eq. (I.1) in terms of rescaled wave functions we obtain

$$\epsilon_{nl} \phi_{\ell} = \frac{1}{S} \left(-\phi_{nl}'' - \frac{2}{z} \phi_{nl}' + \frac{l(l+1)}{z^2} \phi_{nl} \right) - w(z) \phi_{\ell}, \quad (\text{I.13})$$

where

$$\epsilon_{nl} = \frac{1}{S} 2m_a R^2 E_{nl} \quad (\text{I.14})$$

and where the dimensionless halo size parameter is

$$S = 2MGRm_a^2. \quad (\text{I.15})$$

As the expectation value of the kinetic term is positive, Eq. (I.13) implies that the range of the scaled energy parameter is $-1 \leq \epsilon \leq 0$.

Rough estimates show that $S \gg 1$ even for moderate size galaxies, even if the ULA mass is as small as $m_a = 10^{-22}$ eV. For the Milky Way $S_{MW} \gtrsim 10^5$. As a contrast to the galactic halo, $S = O(1)$ for a soliton, or axion star.

Using Eq. (I.13) we estimate the number of bound states. The depth of the rescaled potential well is $w(0) = 1$ and as we see later the spectrum of ϵ_{nl} fills most of the interval $-1 \leq \epsilon \leq 0$. As we will see in the next section, WKB quantization implies that ϵ is quantized as $\epsilon \sim -n/\sqrt{S}$, where n is the principal quantum number. Then the principal quantum number takes up to $O(\sqrt{S})$ different values. Including states with nonzero angular momentum, we estimate that the number of energy levels in the potential well is $O(\sqrt{S})$, a very large number. We find no reason why most of those states would not be occupied by the astronomical number of ULAs. In a previous study [31, 37], only a small number of excited states were considered.

II. WKB APPROXIMATION

Eq. (I.13) lends itself to a perturbative WKB expansion in $\delta = 1/\sqrt{S}$ [38] which gives a solution to the differential equation,

$$\phi_{nl}(z) = \text{Exp} \left[\frac{1}{\delta} \sum_{k=0}^{\infty} \delta^k P_k \right], \quad (\text{II.1})$$

where for the two independent solutions in the allowed, oscillating region are

$$P_0 = \pm i \int_{z_{\min}}^z dz' \sqrt{F_{nl}(z')}, \quad (\text{II.2})$$

$$P_1 = \log \left[\frac{\mathcal{N}_{nl}}{z F_{nl}(z)^{1/4}} \right] \quad (\text{II.3})$$

while terms P_2, \dots are of $O(S^{-1/2})$, and negligible. Eq.(I.13) is linear, so any linear combination of solutions is admissible. The unique solution satisfying boundary conditions, finiteness at the turning points, which are zeros of $F_{nl}[z]$, is

$$\phi_{nl} = \frac{\mathcal{N}_{nl}}{z F_{nl}(z)^{1/4}} \sin \left(\sqrt{S} \int_{z_{\min}}^z dz' \sqrt{F_{nl}(z')} \right), \quad (\text{II.4})$$

where $F_{nl}(z)$ is

$$F_{nl}(z) = w(z) + \epsilon_{nl} - \frac{l(l+1)}{z^2 S}. \quad (\text{II.5})$$

Note that wave functions $\phi_{nl}(z)$ are normalized to 1. Multiplier \mathcal{N}_{nl} is introduced to ensure the correct normalization of wave functions,

$$\mathcal{N}_{nl}^{-2} = 2\pi \int_{z_{\min}}^{z_{\max}} \frac{dz}{F_{nl}(z)^{1/2}}. \quad (\text{II.6})$$

In the classically forbidden region the wave function decreases exponentially as $\phi \propto \exp(-\sqrt{S}c)$, where c is finite as $S \rightarrow \infty$. In the limit $S \rightarrow \infty$ the approximate solution Eq. (II.4) becomes exact. As usual, z_{\min} and z_{\max} are the turning points where $F_{nl} = 0$ (II.4) is also known as the Wentzel ansatz to the WKB solution of Eq. (I.13).

Noting that in Eq. (II.4), factors other than the exponential function vary slowly as function of n and l , the quantization condition for energy eigenvalues ϵ_{nl} can be read off from Eq. (II.4) [39, 40]:

$$\int_{z_{\min}}^{z_{\max}} \sqrt{F_{nl}} = \frac{n}{\sqrt{S}} \pi. \quad (\text{II.7})$$

The principal quantum number, n , and the orbital quantum, l , only appear in combinations $\nu = n/\sqrt{S}$ and $\lambda = (l + 1/2)/\sqrt{S}$.¹ As the separation of subsequent values of quantum numbers ν and λ vanishes as S increases, they will be replaced by continuous variables. That replacement will facilitate the construction of the density as a function of $w(z)$ in the next section. Using the continuous quantum numbers, we can write the wave function as

$$\phi_{\epsilon\lambda} = \frac{\mathcal{N}_{\epsilon\lambda}}{zF_{\epsilon\lambda}(z)^{1/4}} \sin\left(\sqrt{S} \int_{z_{\min}}^z dz' \sqrt{F_{\epsilon\lambda}(z')}\right), \quad (\text{II.8})$$

In Eq. (II.8) we use an unique connection between quantum numbers ν and ϵ through quantization condition (II.7), as it will be explained in the next section.

III. CONSTRUCTION OF THE HALO

The rescaled wave function of the halo is obtained from Eq. (I.2) as

$$\Phi(z, t) = \sum_{nlm} \phi_{nl}(z) Y_{lm}(\theta, \phi) e^{i(\alpha_{nlm} + \epsilon_{nl}t)}. \quad (\text{III.1})$$

Then the total density, averaged over rotations and random phases, and normalized to 1, is

$$\rho(z) = |\Phi(z, t)|^2 \simeq \sum_{nl} (2l + 1) \frac{M_{nl}}{M} |\phi_{nl}|^2. \quad (\text{III.2})$$

Consider now that wave functions depend on quantum numbers n and l only through combinations $\nu = n/\sqrt{S}$, in Eq. (II.7) and $\lambda = \sqrt{l(l+1)}/\sqrt{S}$, in Eq. (II.5). The rescaled quantum numbers, ν and λ , have finite ranges and become dense in those ranges as $S \rightarrow \infty$. Therefore, the error of turning summations over n and l into integrations over ν and λ is only of $O(1/\sqrt{S})$ and negligible for almost all galaxies. Then we obtain

$$\rho(z) = S^{3/2} \int d\nu \int d\lambda^2 \frac{\mathcal{N}_{\epsilon\lambda}^2}{z^2 F_{\epsilon\lambda}^{1/2}} b(\epsilon, \lambda), \quad (\text{III.3})$$

where dimensionless, continuous distribution function $b(\epsilon, \lambda)$ *interpolates distribution function* M_{nl}/M . It is normalized as

$$S^{3/2} \int d\nu \int d\lambda^2 b(\epsilon, \lambda) = 1. \quad (\text{III.4})$$

The total variation of ϵ is 1, or $1 + \epsilon_c$, in case there is a gap of size $|\epsilon_c|$. There are $O(\sqrt{S})$ energy levels, implying that the discrete values of ϵ are dense on interval $(-1, 0)$. Wave functions depend explicitly on ϵ only, therefore we change integration variable ν to ϵ . We use the quantization condition (Eq. (II.7)), written in terms of continuous quantum numbers,

$$\nu \pi = \int_{z_{\min}}^{z_{\max}} dz \sqrt{w[z] + \epsilon - \frac{\lambda^2}{z^2}}, \quad (\text{III.5})$$

to find the appropriate Jacobian. Taking the derivative of Eq. (III.5) with respect to ϵ at constant λ , we note that terms coming from differentiating the integral with respect to boundary values z_{\min} and z_{\max} vanish. Then using Eq. (II.6) we obtain

$$\frac{d\nu}{d\epsilon} \pi = \frac{1}{2} \int_{z_{\min}}^{z_{\max}} \frac{dz}{\sqrt{w(z) + \epsilon - \frac{\lambda^2}{z^2}}} = \frac{1}{4\pi} \mathcal{N}_{nl}^{-2}, \quad (\text{III.6})$$

Substituting Eq. (III.6) into Eq. (III.3) we arrive at our final result for the density:

$$\rho(z) = \frac{S^{3/2}}{4\pi^2} \int_{-w(z)}^{\epsilon_{\max}} d\epsilon \int_0^{z^2(w(z)+\epsilon)} \frac{d\lambda^2 b(\epsilon, \lambda)}{z^2 \sqrt{w[z] + \epsilon - \frac{\lambda^2}{z^2}}}, \quad (\text{III.7})$$

¹ We use Langer's method to define λ [39][40].

where $\epsilon_{\max} \leq 0$ is an admissible integration constant allowing for the existence of an energy gap. If the distribution function $b(\epsilon, \lambda)$ is independent of the angular momentum quantum number, λ , integration over λ yields

$$\rho(z) = \frac{S^{3/2}}{2\pi^2} \int_{-w(z)}^{\epsilon_{\max}} d\epsilon \sqrt{w[z] + \epsilon} b(\epsilon) = \rho(0) \frac{\int_{-w(z)}^{\epsilon_{\max}} d\epsilon \sqrt{w(z) + \epsilon} b(\epsilon)}{\int_{-1}^{\epsilon_{\max}} d\epsilon \sqrt{1 + \epsilon} b(\epsilon)}. \quad (\text{III.8})$$

Even if $b(\epsilon, \lambda)$ depends on λ it is expected that that an expansion with respect to λ^2 converges rapidly. Then, using the expansion

$$b(\epsilon, \lambda) = \sum_{k=0} b(\epsilon)^{(k)} \lambda^{2k} \quad (\text{III.9})$$

we can integrate the series with respect to λ^2 , term by term to obtain

$$\rho(z) = \frac{\rho(0)}{2} \frac{\sum_k z^{2k} \frac{\sqrt{\pi} \Gamma(1+k)}{\Gamma(3/2+k)} \int_{-w(z)}^{\epsilon_{\max}} d\epsilon b^{(k)}(\epsilon) (w(z) + \epsilon)^{k+1/2}}{\int_{-1}^{\epsilon_{\max}} d\epsilon \sqrt{1 + \epsilon} b(\epsilon)} \quad (\text{III.10})$$

Using Eqs. (III.8) or (III.10), the Poisson equation,

$$w''(z) + \frac{2}{z} w'(z) = -4\pi \rho(z) \quad (\text{III.11})$$

becomes a differential equation for $w(z)$. Since $w(0) = 1$ and $w'(0) = 0$, to insure that the density is regular at the center (the exception is the case when density is replaced by the NFW profile), after providing a distribution function there are no undetermined integration constants, other than ϵ_{\max} and $\rho(0)$. As we will see in Sec. V, for some distribution functions $b(\epsilon, \lambda)$ the density (Eq. (III.7)) or (III.8), as appropriate, can be analytically integrated.

The strategy for solving Eq. (III.11) is simpler for Eq. (III.8) than for Eq. (III.10), because after rescaling z as $x = z \sqrt{\rho(0)}$, eliminating the central density from the equation, we find a unique solution at fixed ϵ_{\max} . Among others, we find $\langle 1/x \rangle$. Then we can restore the original scaling variable $z = x \langle 1/x \rangle$, which is true because $\langle 1/z \rangle = 1$. We also find $\rho(0) = \langle 1/x \rangle^2$.

It is more complicated to find the solution of Eq. (III.11) in the case when the energy spectrum is not degenerate. Then, due to the explicit dependence of $\rho(z)$ on z , coordinate z cannot be eliminated from Eq. (III.10) by a simple rescaling. In that case, rather than rescaling z we need to search for an appropriate value of $\rho(0)$ at fixed ϵ_{\max} , such that $\rho(z)$ is normalized to 1.

Dynamical simulations generate numerical distribution functions, as well [30]. A time dependent version of this work, to be published, can potentially do that as well. One advantage of our analytic approximation method is scalability: dynamical simulations are limited by computational power to relatively small galactic halos.

Finally, we note that rotation curves have simple scale invariant representations in terms of our scaling variable and scaling function. Up to an overall factor of dimension of velocity, v_0 ,

$$v(r) = v_0 \sqrt{-z w'(z)}. \quad (\text{III.12})$$

IV. VIRIAL THEOREM IN WKB

Simulations show that, in agreement with expectations, the halo is virialized after collapse [17][18]. Using *stationary* WKB wave functions the halo does not automatically satisfy the virial theorem. However, a time dependent generalization of the WKB approximation is expected to converge to a virialized state. Such a generalization is deferred to a future publication.

The virial theorem for a self-gravitating system, without contact interactions, is $2K + E_g = 0$, where K is the total kinetic energy and V_g is the total gravitational energy. Using the definitions of the previous sections, they are

$$K = \frac{1}{2m_a^2} \sum_{nl} (2l+1) \int d^3r \left[|\psi'_{nl}(r)|^2 + \frac{l(l+1)}{r^2} |\psi_{nl}(r)|^2 \right], \quad (\text{IV.1})$$

$$E_g = \frac{1}{2m_a} \sum_{nl} (2l+1) \int d^3r |\psi_{nl}(r)|^2 V_g(r), \quad (\text{IV.2})$$

where $V_g(r)$ has been defined in Eq. (I.3). Using the dimensionless wave functions and rescaled radial parameter, $z = r/R$, we can rewrite K and V as

$$K = \frac{1}{2m_a^2 R^2} \sum_{nl} (2l+1) M_{nl} \times \int d^3z \left[\phi'_{nl}[z]^2 + \frac{l(l+1)}{z^2} |\phi_{nl}(z)|^2 \right], \quad (\text{IV.3})$$

$$E_g = -\frac{MG}{2R} \sum_{nl} (2l+1) M_{nl} \int d^3z |\phi_{nl}(z)|^2 w(z) \quad (\text{IV.4})$$

Finally, using Eq. (II.8), introducing continuous energy and angular momentum variables as in Eq. (III.3), and expressing G by size parameter S , we obtain

$$K = 2C \int dz \int_{-w(z)}^{\epsilon_c} d\epsilon \int_0^{z^2[w(z)+\epsilon]} d\lambda^2 b(\epsilon, \lambda) \left[\sqrt{w(z) + \epsilon - \frac{\lambda^2}{z^2}} + \frac{\lambda^2}{z^2 \sqrt{w(z) + \epsilon - \frac{\lambda^2}{z^2}}} \right], \quad (\text{IV.5})$$

$$E_g = -C \int dz \int_{-w(z)}^{\epsilon_c} d\epsilon \int_0^{z^2[w(z)+\epsilon]} d\lambda^2 b(\epsilon, \lambda) \frac{w(z)}{\sqrt{w(z) + \epsilon - \frac{\lambda^2}{z^2}}}, \quad (\text{IV.6})$$

where $C = SM/(4m_a^2 R^2)$, is a constant and $\epsilon_c \leq 0$ is an admissible energy cutoff parameter. Then the virial theorem applied to our system becomes independent of all dimensional parameters and of dimensionless size parameter, S . It reads as

$$\int_9^{z_{\text{vir}}} dz z^2 \int_{-w(z)}^{\epsilon_c} d\epsilon \int_0^{z^2[w(z)+\epsilon]} d\lambda^2 \frac{b(\epsilon, \lambda)(3w(z) + 4\epsilon)}{\sqrt{w(z) + \epsilon - \frac{\lambda^2}{z^2}}} = 0. \quad (\text{IV.7})$$

In the particular case when distribution function, $b(\epsilon, \lambda) \rightarrow d_\epsilon$ is independent of λ , we can integrate over λ and the virial theorem becomes

$$\int_9^{z_{\text{vir}}} dz z^2 \int_{-w(z)}^{\epsilon_c} d\epsilon b(\epsilon) \sqrt{w(z) + \epsilon} (3w(z) + 4\epsilon) = 0. \quad (\text{IV.8})$$

Suppose now that an ansatz for the distribution function $b(\epsilon, \lambda)$ depends on a free parameter. A simple example is, ϵ_{max} , defining a gap in the energy spectrum, $b(\epsilon, \lambda) = 0$ for $\epsilon_{\text{max}} < \epsilon < 0$. Another possibility is that a background density, ρ_0 , of undetermined size is subtracted from the density. Then, using the procedure described in Sec. III, we find the numerical gravitational scaling function, $w(z)$, as a function of ϵ_{max} or ρ_0 . Substituting into Eq. (IV.7) allows us to fix ϵ_{max} or, alternatively, ρ_0 , which we will demonstrate in the next section. If there is no choice for the free parameter to satisfy the condition given by Eq. IV.7, then the distribution function $b(\epsilon, \lambda)$ does not allow for the system to reach dynamical equilibrium and is not physically acceptable.

V. EXAMPLES FOR HALOS

To complete the calculation of the density (Eq. (III.7)) we have to know the energy distribution function $b(\epsilon, \lambda)$. In this section we will explore a variety of physical choices for $b(\epsilon, \lambda)$ to check whether they provide acceptable density distributions. In particular, we will pay particular attention to whether the obtained density distribution are in agreement with the following general features of observational data and simulations.

- It is generally accepted [16][13][18] that after its collapse, at least asymptotically in time, the halo is virialized, i.e. satisfies virial condition, $2K + E_g = 0$. In simulations the system is driven towards dynamical equilibrium. As we pointed out earlier, unlike in simulations, $b(\epsilon, \lambda)$ must have a parameter, which can be chosen such that the condition is satisfied.
- Another important feature is that galaxies and galaxy clusters are coming in a very wide range of sizes. As condensation c controls the size of the halo, general solutions must have solutions for a large range of c . However, not all density distributions satisfy this criterion, as an example, a model which we examined in a previous work [42].
- Popular models for galactic halos predict that the rotation curves are independent of the concentration. Though all observed rotation curves are close to being flat, significant variations have been observed [41]. This is especially important if one tries to describe a wide variety halos, including galaxy clusters.

A. Thermal equilibrium

Recently, we applied the WKB expansion method to investigate a system in thermal equilibrium [42]. We give a simplified account of those investigations, below. Neglecting gravitational interactions, the system is treated as an ideal Bose-Einstein gas. The number of particles on energy levels E_n is N_n . Then the partition function for the for the system is

$$e^{-\beta g} = \prod_n \frac{1}{1 - e^{-\beta(E_n - \mu)}}. \quad (\text{V.1})$$

The average value of N_n is

$$\langle N_n \rangle = \frac{1}{e^{\beta(E_n - \mu)} - 1} \quad (\text{V.2})$$

The occupation number, $\langle N_n \rangle$, is enormous in every state, n . As a result, every exponent must satisfy the inequality $1 \gg \beta(E_n - \mu) > 0$. Consequently, we can expand them, keeping terms to linear order, to arrive at the Rayleigh-Jeans limit of Bose-Einstein statistics.

$$\langle N_n \rangle = \frac{1}{\beta(E_n - \mu)} \quad (\text{V.3})$$

Using Eq. (I.13) and rescaling β and μ as

$$\begin{aligned} \beta &= \frac{2m_a R^2}{S} \tilde{\beta}, \\ \mu &= \frac{S}{2m_a R^2} \tilde{\mu} \end{aligned} \quad (\text{V.4})$$

we substitute into Eq. (III.8), to get

$$\rho(z) = \rho_0 \left(\int_{-w(z)}^0 \frac{\sqrt{w(z) + \epsilon}}{\epsilon - \tilde{\mu}} d\epsilon - \rho_B \right), \quad (\text{V.5})$$

where

$$\rho_0 = \frac{S^{3/2}}{4\pi^2 \tilde{\beta}}$$

and $\rho_0 \rho_B$ is a background density term. ρ_B is considered to be an adjustable parameter.

Now remember that the ground state corresponds to $\epsilon = -1$, Then the physical range of the chemical potential is $\tilde{\mu} \leq -1$. During the collapse of the halo the system cools and the chemical potential increase towards its critical value, $\tilde{\mu} = -1$, where Bose-Einstein condensation starts. Integrating density $\rho(z)$ and setting $\tilde{\mu} = -1$ we obtain Poisson equation

$$\begin{aligned} w''(z) + \frac{2}{z} w'(z) &= -8\rho_0\pi \\ \left[\tan^{-1} \left(\sqrt{\frac{w(z)}{1-w(z)}} \right) \sqrt{1-w(z)} - \sqrt{w(z)} - \frac{\rho_B}{2} \right]. \end{aligned} \quad (\text{V.6})$$

To facilitate the numerical solution of Eq. (V.6) we rescale coordinate $z \rightarrow x/\sqrt{8\rho_0\pi}$. Then integrating the Poisson equation at a series of choices for background density parameter ρ_B , we find that at $\rho_B = 0.017$, the virial condition (Eq. (IV.8)) is satisfied. As at that choice of ρ_B $w(x_{\text{vir}}) = 0$, where $x_{\text{vir}} \simeq 4.74$. We also calculate the concentration,

$$c = \left\langle \frac{1}{x} \right\rangle x_{\text{vir}} \simeq 2.78$$

A similar value is obtained for c if we modify the distribution function to take into account gravitational interactions. That can be done by replacing energy level E_n by H_n , the contribution of that energy level to the conserved Hamiltonian. Since observations imply $c \gtrsim 10$, the final state of the collapse cannot be in dynamical equilibrium and thermal equilibrium at the same time.

B. The King model

The King model [43] is based on the classical kinetic theory of collision-free self-gravitating particles, assuming Maxwell velocity distribution cut off at an escape velocity. Then the equilibrium energy distribution takes the form

$$f_{\text{King}} = \begin{cases} A (e^{-\beta(E-E_c)} - 1) & \text{if } E \leq E_c \\ 0 & \text{otherwise.} \end{cases} \quad (\text{V.7})$$

In a recent paper, [30], galactic halos were constructed, using the King distribution [43] (and other classical distribution functions, like the fermionic King model and the Ossipov-Merritt model [44, 45]), combined by wave functions of excited states of Eq. I.1 obtained by simulations. The halos were compared to profiles obtained by simulations of collapsing systems of ultralight bosons, with excellent agreement. Unlike in [30], we do not add a contribution for the condensate at the core of the density distribution, because our aim is to compare the densities predicted by the King model to phenomenological models, rather than the results of simulations. However, our result are in excellent agreement with simulations outside of the $z \lesssim 0.1$ region where the soliton core dominates the density distribution.

We will use our analytic WKB wave functions (Eq. (II.8)) combined with the King distribution function to construct halos, which reduces the number of parameters used in the construction. The fermionic King model, also used in [30] give slightly better fits, as it has an extra adjustable parameter. As we will see below, using WKB wave functions, rather than simulations, has the advantage of scalability, which allows us to find new features when investigating larger systems.

Adapting Eq. (V.7) to WKB wave functions we write Eq. (III.8) as

$$\rho(z) = \frac{AS^{3/2}}{4\pi^2} \int_{-w(z)}^{\epsilon_c} d\epsilon \left(e^{-\beta(\epsilon-\epsilon_c)} - 1 \right) \sqrt{w[z] + \epsilon}, \quad (\text{V.8})$$

Scaling out coefficient $A(S/\beta)^{3/2}/4\pi^2$ from the density and rescaling $z \rightarrow x$, as explained in Sec. III, we integrate over ϵ to get the Poisson equation

$$\begin{aligned} q''(x) + \frac{2}{x}q'(x) \\ = -3 \left[e^{q(x)} \text{erf} \left(\sqrt{q(x)} \right) - 6\sqrt{q(x)} - 4q(x)^{3/2} \right], \end{aligned} \quad (\text{V.9})$$

where

$$q(x) = \beta(w(z) + \epsilon_c), \quad (\text{V.10})$$

and where

$$x = z \frac{A^{1/2}S^{3/2}}{2\sqrt{6\pi}\beta^{1/4}}. \quad (\text{V.11})$$

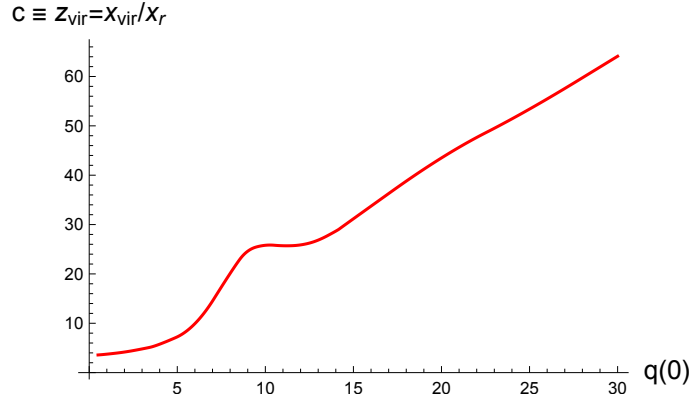
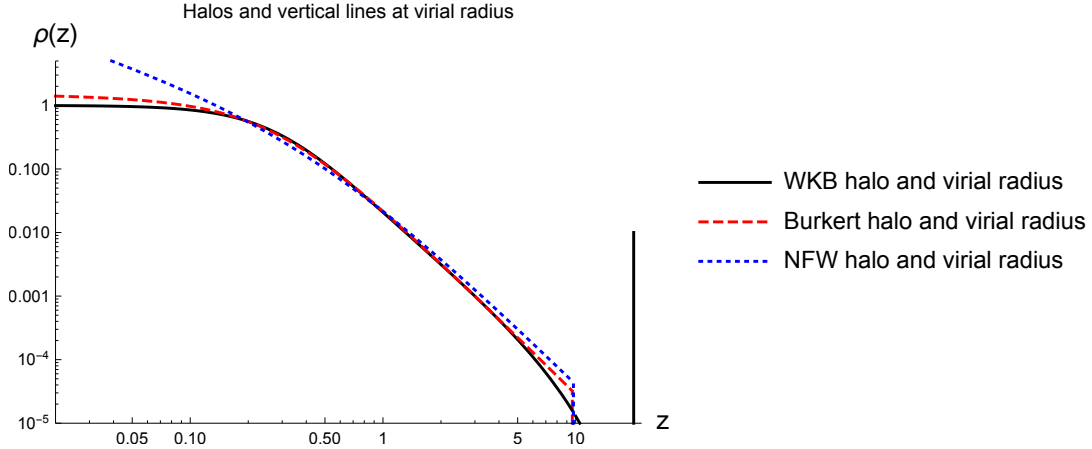
The only adjustable parameter in the Poisson equation (Eq. (V.9)) is $q(0) = \beta(1 + \epsilon_c)$, which we took be to a number of values. We found that the concentration, $c = z_{\text{vir}} = x_{\text{vir}}(1/x)$, plotted in Fig. 1, is a rapidly rising function of $q(0)$. The implication is that the King model can describe halos of markedly different sizes.

We found that in the range $7 \lesssim q(0) \lesssim 10$, the King model density distributions are quite close to NFW or Burkert distributions well in the region where the bulk of the density is distributed, $0.1 \lesssim z \lesssim 10$. As an example, we plot the WKB density distribution, $\rho(z)$, corresponding to initial condition $q(0) = 8$ in Fig. 2. We switch to the physical, rescaled radial coordinate, z and choose central density $\rho(0) = 1$ in the plot. NFW and Burkert profiles, the core density and core radius parameters of which were fitted to the numerically calculated halo, are also plotted. We found fitted parameters $R_{\text{NFW}} = 0.437R$, and $R_{\text{Burkert}} = 0.269R$, where R is the harmonic radius of the WKB solution. Then, we were able to calculate the virial radii and concentrations of those profiles using Eqs. (I.9) and (I.10). We found $c_{\text{NFW}} = 22.3$ and $c_{\text{Burkert}} = 35.7$ and physical virial radii,

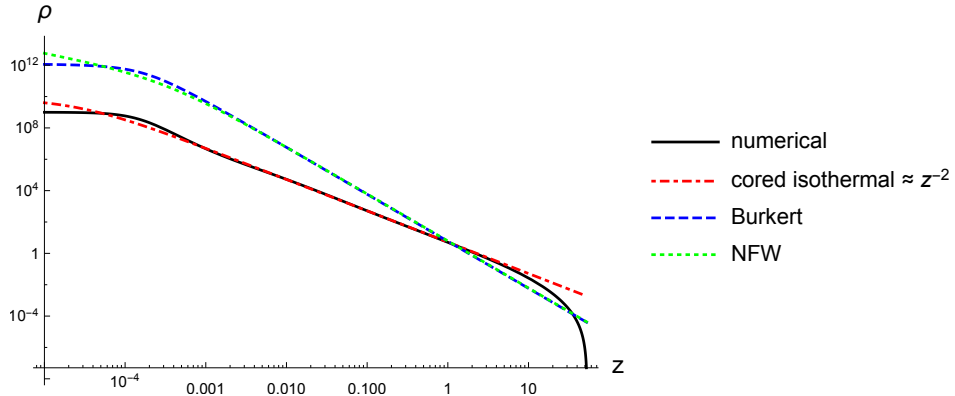
$$\begin{aligned} z_{\text{NFW}} &= c_{\text{NFW}}R_{\text{NFW}}/R = 9.78, \\ z_{\text{Burkert}} &= c_{\text{Burkert}}R_{\text{Burkert}}/R = 9.74, \end{aligned} \quad (\text{V.12})$$

which are quite close to each other. The virial radius of the WKB halo is $z_{\text{vir}} = 20.1$, as it does not have a sharp cutoff. However, in the region $10 < z < 20$, $\rho(z) = \mathcal{O}(10^{-5})$.

Next, we examine the predictions of the King model at a larger virial radius, in the range where c is a linearly rising function of $q(0)$, as it can be seen in Fig. 1. Very likely that range corresponds to galaxies larger than the Milky Way,

FIG. 1: Virial radius as a function of $q(0)$ FIG. 2: King model density distribution compared to NFW and Burkert profiles at $q(0) = 8$.

or galaxy clusters, which are currently not accessible for simulations. At $q(0) \gtrsim 12$ density profiles are very different from those at $q(0) = 8$, plotted in Fig. 3. In fact, they are in excellent agreement with a slightly cored isothermal profile, with behavior $\rho(z) \propto z^{-2}$. We plot $\rho(z)$ at $q(0) = 25$ as a function of z in Fig. 3, along with a weakly cored pseudo-isothermal profile, an NFW profile, and a Burkert profile. All profiles are scaled to match at $z = 1$, which corresponds to the harmonic average radius of the system. Note that the bulk of contributions to the total mass come from the range $0.01 \lesssim z \lesssim 10$.

FIG. 3: King model density distribution compared to isothermal, NFW and Burkert profiles at $q(0) = 25$.

Clearly, the King model profile is in excellent agreement with the isothermal profile [46][47][48][49], while the NFW and Burkert profiles are not.

Lin et. al. [30] generated two halos labeled A and B, for which they fit energy cutoff parameter, E_c and scale parameter, β_{sim} , defining the King model. We wish to compare those with parameters we use to construct WKB halos. However, the corresponding values of β_{WKB} and ϵ_c cannot be directly compared with the simulations of [30], because we rescaled energy $E \rightarrow \epsilon$ and, consequently, our β value is also rescaled, though rescaling leaves the dimensionless quantity $E_c \beta_{\text{sim}} = \epsilon_c \beta_{\text{WKB}}$, unchanged. To check that equality, we need to use the relationship (Eq. (V.10)), which implies of $q(0) = \beta_{\text{WKB}}(1 + \epsilon_c)$. Note now, that cutoff parameter ϵ_c has not been fixed in previous calculations. In other words, ϵ_c is a free parameter.

Consider now that the halos generated in [30] are virialized, while there is no reason why our halos would in general be. In fact, calculating (IV.8) as

$$2K + E \propto \int_0^{z_{\text{vir}}} dz z^2 \int_{-w(z)}^{\epsilon_c} d\epsilon \sqrt{w(z) + \epsilon} \times \left(e^{-\beta(\epsilon - \epsilon_c)} - 1 \right) \left(\epsilon + \frac{3}{4}w(z) \right) \quad (\text{V.13})$$

we find that at every $q(0)$ we have $\langle 2K + E \rangle = a + b\beta\epsilon_c$ with varying fixed values for a and b . Then the vanishing of $\langle 2K + E \rangle$ fixes the combination $\beta\epsilon_c$ at every choice of $q(0)$.

We plot the combination $\epsilon_c\beta$ as function of $q(0)$ along with the values of $E_c\beta_{\text{sim}}$ of halos A and B, -0.539 and -0.51 , of [30], in Fig. 4. Those combinations are equal after rescaling E_c and β . The deviation of values of $\beta\epsilon_c$ between those found in our WKB calculation and those in simulations, are only a few percent at the relevant values of $q(0)$.

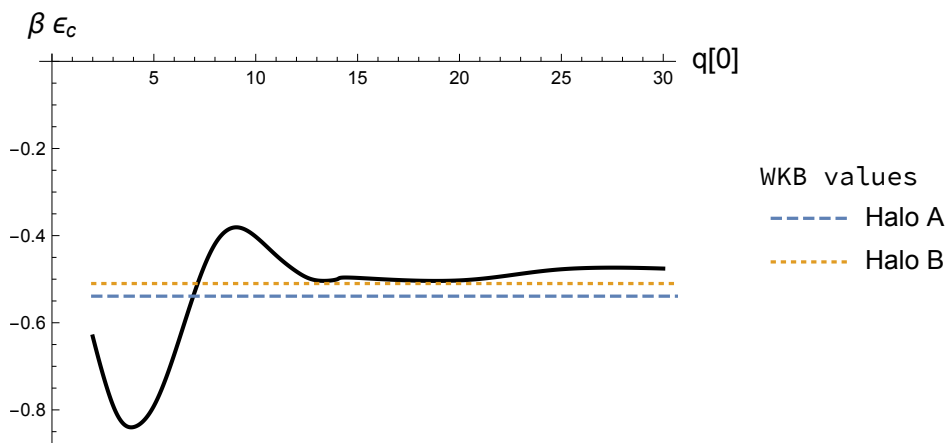


FIG. 4

Plot of King model values of $\beta\epsilon_c$ along with those of halos A and B obtained in simulations of [30].

VI. SUMMARY

We have investigated the possibility that galactic dark matter haloes could be made up of ultra-light bosons with wave functions that satisfy nonlinear Schrodinger-Poisson equations. We have found eigenstates and eigenvalues of the Schrodinger equation using the WKB approximation. The approximation method becomes more accurate as the galaxy's mass rises, however it has been demonstrated that even for smaller galaxies, the leading WKB approximation may yield accurate answers. The WKB approximation expresses the wave functions in terms of the gravitational potential. The energy levels were determined by the Bohr-Sommerfeld quantization condition, implied by the WKB method. To determine how we may better explain the data we have compared two anätze for the level occupation number distributions, the Bose-Einstein distribution and the King model, at appropriate values of temperature and chemical potential. The modulus square of each wave function multiplied by the occupation number, summed over all the bound states, yielded the total density of particles. The mass density is therefore a function of the gravitational potential V_g since the Poisson equation connects V_g to the particle density. This procedure allowed us to obtain a differential equation for the gravitational potential. Solving this equation enabled us to obtain the mass distribution of the ULDM model of a galaxy. This technique can easily be scaled up to model the DM halos of galaxies or galaxy clusters, well beyond the mass range covered by simulations.

When we used the Bose Einstein density distribution in our computation of the density profile we observed that the concentration parameter, c , of the resulting galaxy was smaller in magnitude than what is observed for most galaxies.

When the King model particle distribution was utilized the concentration parameters, on the other hand, were within the permissible range for Milky way-like galaxies.

In future work we plan to study the dynamical collapse of boson clouds using variational technique and study the times scales for collapse and decay in more detail. We will also investigate how the inclusion of self-interactions affects the the dynamics of halo.

ACKNOWLEDGMENTS

The authors are indebted to Joshua Eby for fruitful discussions. L.S. also thanks the Department of Physics at the University of Cincinnati for financial support in the form of the Violet M. Diller Fellowship. During part of this research L.S. was supported by the U.S. Department of Energy (DOE), Office of Science, Office of Workforce Development for Teachers and Scientists, Office of Science Graduate Student Research (SCGSR) program. The SCGSR program is administered by the Oak Ridge Institute for Science and Education (ORISE) for the DOE. ORISE is managed by ORAU under contract number DE-SC0014664. All opinions expressed in this paper are the authors' and do not necessarily reflect the policies and views of DOE, ORAU, or ORISE. Research of L.C.R.W. is partially supported by the US. Department of Energy grant DE-SC1019775.

-
- [1] P. J. E. Peebles, *Large-scale background temperature and mass fluctuations due to scale-invariant primeval perturbations*, *AstroPhys. J.* **263** (1982) L1.
- [2] J. R. Bond, A. S. Szalay and M. S. Turner, *Formation of Galaxies in a Gravitino Dominated Universe*, *Phys. Rev. Lett.* **48** (1982) 1636.
- [3] G. R. Blumenthal, H. Pagels and J. R. Primack, *Galaxy Formation by Dissipationless Particles Heavier than Neutrinos*, *Nature* **299** (1982) 37.
- [4] M. R. Baldeschi, R. Ruffini and G. B. Gelmini, *On Massive Fermions and Bosons in Galactic Halos*, *Phys. Lett. B* **122** (1983) 221.
- [5] M. S. Turner, *Coherent Scalar Field Oscillations in an Expanding Universe*, *Phys. Rev. D* **28** (1983) 1243.
- [6] W. H. Press, B. S. Ryden and D. N. Spergel, *Single Mechanism for Generating Large Scale Structure and Providing Dark Missing Matter*, *Phys. Rev. Lett.* **64** (1990) 1084.
- [7] S.-J. Sin, *Late time cosmological phase transition and galactic halo as Bose liquid*, *Phys. Rev. D* **50** (1994) 3650 [[hep-ph/9205208](#)].
- [8] W. Hu, R. Barkana and A. Gruzinov, *Cold and fuzzy dark matter*, *Phys. Rev. Lett.* **85** (2000) 1158 [[astro-ph/0003365](#)].
- [9] F. S. Guzman and L. A. Urena-Lopez, *Evolution of the Schrodinger-Newton system for a selfgravitating scalar field*, *Phys. Rev. D* **69** (2004) 124033 [[gr-qc/0404014](#)].
- [10] C. G. Boehmer and T. Harko, *Dark energy as a massive vector field*, *Eur. Phys. J. C* **50** (2007) 423 [[gr-qc/0701029](#)].
- [11] D. H. Weinberg, J. S. Bullock, F. Governato, R. Kuzio de Naray and A. H. G. Peter, *Cold dark matter: controversies on small scales*, *Proc. Nat. Acad. Sci.* **112** (2015) 12249 [[1306.0913](#)].
- [12] D. J. E. Marsh and A.-R. Pop, *Axion dark matter, solitons and the cusp-core problem*, *Mon. Not. Roy. Astron. Soc.* **451** (2015) 2479 [[1502.03456](#)].
- [13] L. Hui, J. P. Ostriker, S. Tremaine and E. Witten, *Ultralight scalars as cosmological dark matter*, *Phys. Rev. D* **95** (2017) 043541 [[1610.08297](#)].
- [14] J.-W. Lee, *Brief History of Ultra-light Scalar Dark Matter Models*, *EPJ Web Conf.* **168** (2018) 06005 [[1704.05057](#)].
- [15] E. G. M. Ferreira, *Ultra-light dark matter*, *Astron. Astrophys. Rev.* **29** (2021) 7 [[2005.03254](#)].
- [16] H.-Y. Schive, T. Chiueh and T. Broadhurst, *Cosmic Structure as the Quantum Interference of a Coherent Dark Wave*, *Nature Phys.* **10** (2014) 496 [[1406.6586](#)].
- [17] H.-Y. Schive, M.-H. Liao, T.-P. Woo, S.-K. Wong, T. Chiueh, T. Broadhurst et al., *Understanding the Core-Halo Relation of Quantum Wave Dark Matter from 3D Simulations*, *Phys. Rev. Lett.* **113** (2014) 261302 [[1407.7762](#)].
- [18] B. Schwabe, J. C. Niemeyer and J. F. Engels, *Simulations of solitonic core mergers in ultralight axion dark matter cosmologies*, *Phys. Rev. D* **94** (2016) 043513 [[1606.05151](#)].
- [19] J. Veltmaat and J. C. Niemeyer, *Cosmological particle-in-cell simulations with ultralight axion dark matter*, *Phys. Rev. D* **94** (2016) 123523 [[1608.00802](#)].
- [20] X. Du, C. Behrens, J. C. Niemeyer and B. Schwabe, *Core-halo mass relation of ultralight axion dark matter from merger history*, *Phys. Rev. D* **95** (2017) 043519 [[1609.09414](#)].
- [21] P. Mocz, M. Vogelsberger, V. H. Robles, J. Zavala, M. Boylan-Kolchin, A. Fialkov et al., *Galaxy formation with BECDM – I. Turbulence and relaxation of idealized haloes*, *Mon. Not. Roy. Astron. Soc.* **471** (2017) 4559 [[1705.05845](#)].
- [22] D. G. Levkov, A. G. Panin and I. I. Tkachev, *Gravitational Bose-Einstein condensation in the kinetic regime*, *Phys. Rev. Lett.* **121** (2018) 151301 [[1804.05857](#)].
- [23] P. Mocz et al., *First star-forming structures in fuzzy cosmic filaments*, *Phys. Rev. Lett.* **123** (2019) 141301 [[1910.01653](#)].
- [24] M. A. Amin and P. Mocz, *Formation, gravitational clustering, and interactions of nonrelativistic solitons in an expanding universe*, *Phys. Rev. D* [[1902.07261](#)].
- [25] N. Glennon and C. Prescod-Weinstein, *Modifying PyUltraLight to model scalar dark matter with self-interactions*, *Phys. Rev. D* **104** (2021) 083532 [[2011.09510](#)].
- [26] P. Mocz, A. Fialkov, M. Vogelsberger, M. Boylan-Kolchin, P. H. Chavanis, M. A. Amin, S. Bose, T. Dome, L. Hernquist and L. Lancaster, *et al.* *Mon. Not. Roy. Astron. Soc.* **521**, no.2, 2608-2615 (2023) doi:10.1093/mnras/stad694 [[arXiv:2301.10266](#) [[astro-ph.CO](#)]].
- [27] H. Huang, H.-Y. Schive and T. Chiueh, *Cosmological Simulations of Two-Component Wave Dark Matter*, 2212.14288.
- [28] N. Glennon, N. Musoke and C. Prescod-Weinstein, *Simulations of multifield ultralight axionlike dark matter*, *Phys. Rev. D* **107** (2023) 063520.

- [29] J. Luna Zagorac, I. Sands, N. Padmanabhan, and R. Easther, *Schrödinger-Poisson solitons: Perturbation theory*, *Phys. Rev. D* **105** (2022) 103506. [1103.2054].
- [30] S.-C. Lin, H.-Y. Schive, S.-K. Wong and T. Chiueh, *Self-consistent construction of virialized wave dark matter halos*, *Phys. Rev. D* **97** (2018) 103523 [1801.02320]
- [31] F. S. Guzmán and L. A. Ureña López, *Gravitational atoms: General framework for the construction of multistate axially symmetric solutions of the Schrödinger-Poisson system*, *Phys. Rev. D* **101** (2020) 081302.
- [32] P.-H. Chavanis, *Mass-radius relation of newtonian self-gravitating bose-einstein condensates with short-range interactions. i. analytical results*, *Phys. Rev.D* [2109.01928]
- [33] P. H. Chavanis and L. Delfini, *Mass-radius relation of Newtonian self-gravitating Bose-Einstein condensates with short-range interactions: II. Numerical results*, *Phys. Rev. D* **84** (2011) 043532 [1103.2054].
- [34] J. Eby, P. Suranyi and L. C. R. Wijewardhana, *The Lifetime of Axion Stars*, *Mod. Phys. Lett. A* **31** (2016) 1650090 [1512.01709].
- [35] J. F. Navarro, C. S. Frenk and S. D. M. White, *The Structure of cold dark matter halos*, *Astrophys. J.* **462** (1996) 563 [astro-ph/9508025].
- [36] A. Burkert, *The Structure of dark matter halos in dwarf galaxies*, *Astrophys. J. Lett.* **447** (1995) L25 [astro-ph/9504041].
- [37] A. Bernal, J. Barranco, D. Alic and C. Palenzuela, *Multi-state Boson Stars*, *Phys. Rev. D* **81** (2010) 044031 [0908.2435].
- [38] C. Bender and S. Orszag, *Advanced Mathematical Methods for Scientists and Engineers: Asymptotic Methods and Perturbation Theory*, vol. 1. 01, 1999, 10.1007/978-1-4757-3069-2.
- [39] R. E. Langer, *On the connection formulas and the solutions of the wave equation*, *Phys. Rev.* **51** (1937) 669.
- [40] M. N. Sergeenko, *Semiclassical wave equation and exactness of the WKB method*, *Phys. Rev. A* **53** (1996) 3798.
- [41] A. Zintner, S. Dandavate, O. Slone and M. Lisanti, *A critical Assessment of Solutions to the Galaxy Diversity Problem*, *JCAP* **121** (2018) 151301 [2202.00012v2]
- [42] L. Street, P. Suranyi and L. C. R. Wijewardhana, *Density profile of multi-state fuzzy dark matter*, 2101.00349.
- [43] I. R. King, *The structure of star clusters. III. Some simple dynamical models*, "Astron. J." **71** (1966) 64.
- [44] L. P. Osipkov, *Spherical systems of gravitating bodies with ellipsoidal velocity distribution.*, *Pisma v Astronomicheskii Zhurnal* **5** (1979) 77.
- [45] D. Merritt, *Spherical stellar systems with spheroidal velocity distributions*, "Astron. J." **90** (1985) 1027.
- [46] S. May, V. Springel, *The halo mass function and filaments in full cosmological simulations with fuzzy dark matter* *Monthly Notices of the Royal Astronomical Society/stad2031* [0302.560]
- [47] R. Jimenez, L. Verde, T. Treu and D. Stern, *Constraints on the equation of state of dark energy and the Hubble constant from stellar ages and the CMB* *Astrophys. J.* **593** (2003) 6220 [0302.560]
- [48] C. Shu, B. Zhou, M. Bartemann, J. Comerford, J. Huang and Y. Mellier, *Comparisons between Isothermal and NFW Mass Profiles for Strong-Lensing Galaxy Clusters*, *Astrophys. J.* **685** (2008) 70 [0805.1148]
- [49] J. Brownstein, *Modified Gravity and the Phantom of Dark Matter* [0908.0040v1]